Template

SPECIALTY FIBER TECHNOLOGY FOR BRILLOUIN OPTICAL TIME DOMAIN ANALYSIS

Dora Juan Juan Hu[1*], Hui Dong[1], and Hailiang Zhang[1]

[1]Institute for Infocomm Research (I[2]R), Agency for Science, Technology and Research (A*STAR), 1 Fusionopolis Way, #21-01, Connexis South Tower, Singapore 138632, Republic of Singapore

jjhu@i2r.a-star.edu.sg; hdong@i2r.a-star.edu.sg; zhang_hailiang@i2r.a-star.edu.sg;

Corresponding author: jjhu@i2r.a-star.edu.sg;

Abstract

Brillouin optical time domain analysis (BOTDA) is a powerful technique for measuring the temperature and strain distribution along an optical fiber using Brillouin scattering. It has offered many opportunities in various industries including structural health monitoring for civil infrastructure, oil and gas industry, geophysical exploration, environmental monitoring etc. As the technology of specialty fibers is continuously evolving, it is bringing new and enhanced opportunities for BOTDA applications by enabling new sensing capabilities and addressing specific challenges. For example, specialty fibers with special materials and/or special structures have been applied in BOTDA system to achieve enhanced sensor performance, including large scale strain sensing, temperature-insensitive strain sensing, high temperature strain sensing. These performance enhancements lead to many favourable applications, such as curvature sensing and shape reconstruction, discriminative sensing of temperature and strain. Multiplexed sensing systems have been developed to realize multipurpose sensing capabilities, such as hybrid Brillouin and Rayleigh sensing system, hybrid Brillouin and Raman sensing system. This book chapter introduces the fundamentals of utilization of unique properties of specialty fibers in BOTDA system and highlights specific applications. This book chapter could serve as a useful resource for researchers, engineers, and scientists working in the field of optical sensing and fiber optics.

Introduction

Brillouin scattering, named after the French physicist Léon Brillouin, was theoretically predicted in 1922 (Brillouin, 1922). The stimulated Brillouin scattering (SBS) is a nonlinear process dependent on input power. The backscattered Stokes light interferes with the input pump light and generates an acoustic wave through the effect of electrostriction (Kobyakov, et al., 2010). The Brillouin frequency shift (BFS) is the frequency difference between the Stokes wave and the pump at which the amplification of the Stokes wave is the maximum. BFS depends on the mechanical and thermal conditions of the fiber, i.e., increasing with both strain and temperature, forming the sensing principle of the Brillouin optical time domain analysis (BOTDA) (Kobyakov, et al., 2010). The SBS process in which the acoustic wave generated from the light beam was first observed in 1964 (Chiao, et al., 1964), and was later observed in optical fiber and reported by Ippen et al. in 1972 (E. P. Ippen, 1972). The SBS process was harnessed to develop Brillouin fiber sensors to measure physical parameters (Kobyakov, et al., 2010).

Since the introduction of the BOTDA system in 1990 (T.Horiguchi, et al., 1990), it has undergone rapid development primarily owing to its ability to provide continuous and highly accurate distributed measurement of temperature and/or strain in optical fibers (Bao, et al., 1993; Niklès, et al., 1996). It has gained wide application in various fields, including long term structural health monitoring (SHM) and assessment of infrastructure in civil engineering (Guo, et al., 2009; Liu, et al., 2021; Zhang, et al., 2020), oil and gas pipelines (Kwon, et al., 2009; Zhang, et al., 2019), and geoscience (Iten, et al., 2011; Cao, et al., 2019), just to name a few. To overcome the technical challenges of BOTDA systems such as spatial resolution, sensing range, measurement time etc, various strategies in the sensing interrogators have been proposed and implemented (Bao & Chen, 2011; Motil, et al., 2016; Feng, et al., 2019; Dong, 2021). Besides innovations in the sensing interrogators, an important aspect of research effort is placed and realized in the optical fiber cables for successful exploitation of Brillouin distributed sensing (Bastianini, et al., 2019). Various Brillouin scattering materials have been explored to provide reference and guidance to SBS related experiments and application development (Bai, et al., 2018). Integration of specialty fiber technology into BOTDA system leads to many exciting benefits in sensing performance improvement and opportunities for new sensing applications. There are several ways to explore and design the BOTDA system from the perspectives of fibers (Dragic & Ballato, 2018) or fiber cables (Bastianini, et al., 2019). Firstly, optimization through the optical and acoustic waveguide design of the fibers would result in novel fiber configurations that have potential for discriminative sensing; Secondly, the fiber materials, selections of dopants can enrich the design of the specialty fibers that can provide unconventional properties (Dragic & Ballato, 2018); Lastly, sensing cable is another element that can be designed specifically for Brillouin sensing, including the selection of type, coating, materials, and geometry of the fiber cable component (Bastianini, et al., 2019).

In this chapter, the focus is primarily on specialty fiber based BOTDA systems and applications. Other Brillouin sensing systems, such as Brillouin Optical Time Domain Reflectometry (BOTDR), Brillouin optical correlation-domain analysis (BOCDA) etc., based on specialty fibers, are not discussed within the scope of this chapter. In subsequent sections, the working principle of BOTDA is presented, followed by a brief overview of specialty fiber technologies that are applied in BOTDA systems. Subsequently, the examples of the specialty optical fiber enabled BOTDA systems are presented, including optical fibers with special materials, special structures, and multiplexed fiber sensing systems. An overview of applications enabled by specialty fiber based BOTDA is presented. Lastly, the prospects of using specialty fibers for BOTDA systems are discussed.

BOTDA technology and applications

In a BOTDA system, the Brillouin interaction between a pulsed pump and a counter-propagating continuous wave (CW) probe can be measured by the schematic setup in Fig. 1. The frequency difference between the pulsed and the CW light is turned to the Brillouin frequency of the fiber associated with amplification of the probe light [11]. The probe power is measured as a function of time, which is translated to a distance-dependent information to derive local Brillouin gain. The local BFS at each point of the fiber is derived from reconstruction of Brillouin gain spectrum (BGS) by a frequency sweep with every frequency detuning around the Brillouin frequency.

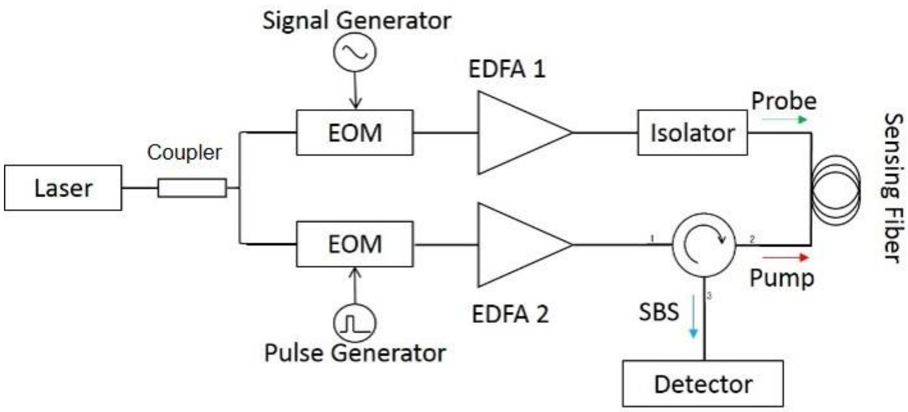

Fig.1. Schematic setup of BOTDA system [Reprinted/Adapted] with permission from (Hu, et al., 2021)

Specialty fibers such as photonic crystal fibers (PCFs) and hollow core fibers are fabricated using silica and other non-silica materials, which introduce various design flexibility in applications (Liu, et al., 2023). Their holey structure is another dimension for waveguide design and properties optimization for sensing performance. Combining the material and the structural tunability, fibers provide an ideal platform to integrate with high gain SBS medium to boost the overall Brillouin amplification (Yang, et al., 2020; Yang, et al., 2020), and/or achieve peculiar functions such as polarization noise suppression (Beugnot, et al., 2007), enhancement of sensitivity through suitable coatings (Gu, et al., 2013; Lu, et al., 2017) etc. Distributed sensing systems such as BOTDA system face crucial challenges in distinguishing between temperature and strain responses. This chapter examines the strategies employed to address this challenge, including the incorporation of specialty fibers such as photonic crystal fibers (PCFs), few mode fibers (FMFs), and multicore fibers into the BOTDA solution. The review delves into the introduction of multiplexed distributed sensing, combining BOTDA technology with other Distributed Fiber Sensing (DFS) technologies like Raman optical time domain reflectometry (R-OTDR) or phase-sensitive optical time-domain reflectometry (φ-OTDR) through the utilization of multi-core fibers and spatial multiplexing. These advancements and opportunities have sparked significant interest, propelling the evolution of specialty fiber based BOTDA systems with notable features and performance improvements, as outlined in the subsequent section providing an overview of specialty fiber technology in BOTDA systems.

BOTDAs with optical fibers of special material: Non-silica materials such as polymer are explored to develop advanced fiber sensors, utilizing their unique properties such as high flexibility, large breakage strain and impact resistance, thus enabling applications that demand large sensitivities, large scale strain sensing etc. (Mizuno, et al., 2021). Besides through waveguide design, the Brillouin scattering characteristics such as frequency shift, spectral linewidth, and Brillouin gain can be widely tuned through intrinsic glass materials (Deroh, et al., 2020).

Compared to silica optical fibers which have a fundamental limitation in flexibilities and often break at relatively small strains of <2%-3%, polymer or plastic optical fibers are attracting great attention to overcome this fundamental issue. The BFS and the Brillouin bandwidth in a perfluorinated graded-index (PFGI) polymer optical fiber (POF) with 120 μm core diameter were characterized as 2.83 GHz and 105 MHz (Mizuno & Nakamura, 2010), showing the potential of the utilization of more economical Photodetectors (PD) and Electronic Spectrum Analyzers (ESA) with reduced bandwidth requirements as compared to standard silica fibers. Furthermore, PFGI Polymer fibers demonstrate better mode coupling efficiency and excellent mode scrambling capability regardless of alignment conditions (Dong, et al., 2014). The temperature and strain sensitivity of the PFGI-POF were experimentally characterized, showing negative values which are -3.5 and -0.2 times as compared to silica fibers for strain-insensitive high accuracy temperature sensing (Mizuno & Nakamura, 2010). However, temperature and strain compensation are necessary for accurate POF-based Brillouin sensing due the cross effect of strain and temperature coefficients in selected strain ranges and temperature range of 32-60 °C. Firstly, in the strain range of 0–1.2%, the temperature coefficient has a linear relationship with strain, with a coefficient of 1.5 MHz/(%·°C). Secondly, in the strain ranges of 0–1.2% and 4.0–9.0%, the corresponding temperature dependencies are linear, with coefficients of 1.5 and –0.3 MHz/(%·°C), respectively. Thirdly, for strains exceeding 13%, temperature sensing without sensitivity to strain becomes a potential option using BFS in POFs (Minakawa, et al., 2017). When large strains are applied on PFGI-POF, the Stokes power drastically drops when the applied strain was larger than ~10%. Meanwhile, the dependance of BFS is highly non-monotonic, posing difficulties in accurately determining strain solely through BFS measurements. For strain range 10-15%, the BFS in PFGI-POF has no strain dependance, making it ideal and practical for temperature sensing (Hayashi, et al., 2012). Another study of BFS hopping phenomenon revealed that BFS abruptly changes from 2.7 GHz to 3.2 GHz due to the strain-induced slimming of the over-cladding layer composed of polycarbonate, triggered by the elastic-to-plastic transition (Hayashi, et al., 2014). Wide dynamic range of strain measurement >25% has been achieved by applying 3.0% strain to a slimmed POF beforehand (Mizuno, et al., 2018).

The BFS dependence on water absorption ratio has been observed in standard fibers, showing nonlinear displacement with hysteretic behavior. Thus, the humidity isolation is a critical factor for achieving precise BFS measurements (Galindez, et al., 2008). In PMMA fibers, the BFS decreased monotonically as the water absorption ratio increased, due to decreasing Young's modulus. Moreover, at the same water absorption ratio, the BFS change was larger at a higher temperature (Minakawa, et al., 2016). The humidity induced BFS in PFGI-POF has been characterized, showing very different characteristics from standard fibers. Firstly, there is a linear relationship between BFS and humidity at constant temperatures. Secondly, there is no hysteresis observed due to humidity changes. Thirdly, the temperature coefficient of BFS is independent of humidity variations. Lastly, an analytical description has been proposed to decouple the temperature and humidity as two mutually independent effects on the BFS, enabling a quantitative estimation of BFS for specified temperature and humidity (Schreier, et al., 2018). The humidity induced BFS was predominantly caused by fiber straining because of swelling of the fiber over-cladding. In addition, PFGI-POFs demonstrate a greater humidity-induced strain response compared to standard silica fibers coated with polyimide and acrylate. The measured strain coefficient of (–146.5±0.9) MHz/% within strain range from 0.1% to 1.5%. The fiber expansion coefficient for humidity and temperatures are $(7.4\pm0.1)\cdot10^{-6}$ %r.h.$^{-1}$ and $(22.7\pm0.3)\cdot10^{-6}K^{-1}$ (Schreier, et al., 2018). The potential of using polymer optical for distributed pressure sensing is reported (Mizuno, et al., 2018), showing a significant pressure sensitivity 4.3 MHz/MPa which is 5.8 times of bare silica fibers with opposite sign. In addition, the hysteresis of the pressure response is mitigated after several cycles of increasing/decreasing pressure.

Tellurite fibers with large Brillouin gain coefficients of 1.7×10^{-10} m/W in BOCDR configuration have been reported to show negative strain coefficient −230 MHz/% and temperature coefficient −1.14 MHz/ °C of the BFS, respectively (Mizuno, et al., 2010; Mizuno, et al., 2009).

Bismuth-oxide nonlinear fibers were demonstrated to have superior Kerr nonlinear efficiency over silica fibers (Lee, et al., 2005). The temperature coefficient of the BFS in Bismuth-oxide nonlinear fibers were measured by BOCDR system, with the value of -0.88 MHz/ °C (Mizuno, et al., 2009).

Rare-earth-doped fibers, such as Erbium-doped fibers (EDFs) with different erbium concentrations of 0.71, 1.2 and 2.28 wtppt and the same cladding, were investigated by Ding et al. (Ding, et al., 2013)

Strong SBS in single mode chalcogenide glass fibers were observed, demonstrating Brillouin gain coefficient one to two orders of magnitude larger than that of fused silica fiber (Abedin, 2005; Florea, et al., 2006; Fortier, et al., 2008). For example, the estimated Brillouin gain coefficient was $(3.9\pm0.4) \times 10^{-9}$ m/W for the As_2S_3 and $(6.75\pm0.35) \times 10^{-9}$ m/W for As_2Se_3 (Florea, et al., 2006), 8×10^{-10} m/W for Ge15Sb20S_{65} chalcogenide glass microstructured fiber made of germanium sulfide glass (Fortier, et al., 2008). Slow and fast light generation based on SBS was demonstrated in As2Se3 chalcogenide fiber, showing Brillouin gain of 43 dB with 60 mW pump power in a 5 m chalcogenide fiber, which results in 37 ns optical delay of a probe Gaussian pulse of 50 ns duration (Song, et al., 2006). Hybrid PMMA- As_2Se_3 microwires demonstrated significant increase in the Brillouin threshold as compared to the As_2Se_3 fibers due to acoustic damping in the PMMA cladding. In addition, hybrid acoustic modes with both shear and longitudinal phonons can be excited in the microwire. The BFS can be widely tuned by changing the microwire diameters (Beugnot, et al., 2014). Strong coupling of forward and backward Brillouin scattering between core and cladding in a 60 cm hybrid As2Se3-PMMA microtapers was observed, generating amplification of Stokes wave at 7.4 GHz due to modulation by guided-acoustic-wave Brillouin scattering, and two peaks from the interaction of the pump with the Stokes wave through SBS at 7.62 GHz and 7.8 GHz (Saxena, et al., 2019). Simultaneous temperature and strain sensing based on a tapered dual-core As2Se3-PMMA fiber was demonstrated through different BFS response in two principal polarization axes. The temperature coefficients are -3.8272 MHz/°C and –3.2202 MHz/°C, and the strain coefficients are -614.3 MHz/% and -346.3 MHz/% (Wang, et al., 2020). Due to low Young's modulus of the As2Se3 core and the high mechanical strength of PMMA cladding, wide dynamic strain range from 0 to

15000 $\mu\varepsilon$ based on Brillouin frequency and linewidth in an 50 cm-long As2Se3-PMMA hybrid microfiber was achieved. No strain memory effect was observed. This study provided compelling evidence and highlighted the potential of using As2Se3-PMMA hybrid microfiber for wide range strain sensing applications (Wang, et al., 2020). The birefringence influence on SBS was investigated in elliptical-core As2Se3-PMMA microfibers. For a fixed ellipticity of 1.108, the decrease in the minor axis of the core diameter from 1.50 μm to 0.87 μm led to increasing group birefringence from ~10^{-3} to ~10^{-2}, and larger BFS difference from ~ 6 MHz to ~30 MHz, associated with broadened BGS from ~ 70 MHz to ~ 140 MHz (Wang, et al., 2021). Distributed temperature and strain sensing based on a nonuniform As2Se3-PMMA tapered fiber with spatial resolution of 1.1 centimeter was demonstrated by Brillouin gain-profile tracing, using differential BGS at each fiber location (Gao, et al., 2022). Saxena et al. reported the calibration of BFS induced by a transverse load on a 60 cm single-mode As2Se3-PMMA microtaper, showing sensitivity of 0.08 MHz/N (Saxena, et al., 2019).

The comparisons of strain and temperature sensitivities of the BFS among different fiber materials, such as silica fibers, non-silica fiber materials including polymer, Tellurite, Bismuth-oxide, Erbium-doped, and As2Se3-PMMA fibers, are listed in Table 1.

Table 1: Comparison of strain and temperature sensitivities of the BFS among different fiber materials

	Strain sensitivity (MHz/%)	Temperature sensitivity (MHz/°C)	Selected reference(s)
Silica fibers	580	1.18	(Horiguchi, et al., 1989; Kurashima, et al., 1990)
Polymer fibers	-121.8	-4.09	(Mizuno & Nakamura, 2010)
Tellurite fibers	−230	−1.14	(Mizuno, et al., 2010)
Bismuth-oxide fibers	NA	-0.88	(Mizuno, et al., 2009)
Erbium-doped fibers	479	0.87	(Ding, et al., 2013)
Dual core As2Se3-PMMA fiber tapers	-614.3 -346.3	-3.8272 -3.3302	(Wang, et al., 2020)

BOTDAs with optical fibers of special structure: Optical fibers with special structures bring new features and flexibilities in controlling and optimizing the optical and acoustic waveguide properties, thus enabling new applications, and enhancing sensing performance in BOTDA systems. To realize discriminative sensing of temperature and strain in BOTDA systems, there are two main approaches, primarily by constructing a sensor matrix of temperature and strain coefficients in the sensing system and based on a combination of using BFS sensing and other parameters sensing.

The sensor matrix is typically formulated as Equation 1, in which $C_{T1,2}$ and $C_{\varepsilon 1,2}$ represent the temperature and strain coefficients, $\Delta \nu_{\mathrm{B\_peak1,2}}$ represent the central frequency shifts of the Brillouin spectra peaks. The temperature change ΔT and the strain change $\Delta\varepsilon$ along the fiber are calculated by solving the inverse matrix problem.

$$\begin{bmatrix} \Delta\nu_{\mathrm{B\_peak1}} \\ \Delta\nu_{\mathrm{B\_peak2}} \end{bmatrix} = \begin{bmatrix} C_{T1} & C_{\varepsilon 1} \\ C_{T2} & C_{\varepsilon 2} \end{bmatrix} \begin{bmatrix} \Delta T \\ \Delta\varepsilon \end{bmatrix} \qquad \text{(Equation 1)}$$

The reported approaches to achieve discrimination of temperature and strain by specialty fiber are summarized in Table 2 (Hu, et al., 2021), including exploiting the multi-peak BGS due to multiple acoustic modes and/or multiple optical modes, multiple core/fibers, BFS and other parameters such as birefringence, fluorescence, and athermal/atensic optical fibers.

Table 2: Summary of reported approaches to achieve discriminative sensing using specialty fibers [Reprinted/Adapted] with permission from (Hu, et al., 2021)

Template

Approaches	Specialty fiber type	Temperature coefficient $C_T\ (MHz/^\circ C)$	Strain coefficient $C_\varepsilon\ (MHz/\mu\varepsilon)$
Multi-peak BGS due to multiple acoustic modes	PCFs with a partially germanium-doped core (Zou, et al., 2003; Zou, et al., 2004) Peak 1 Peak 2	 0.96 1.25	 0.048 0.055
	Large effective-area fiber (LEAF) (Liu & Bao, 2012) Peak 1 BFS Peak 1 BGS linewidth Peak 2 BFS Peak 2 BGS linewidth	 1.18 -0.111 1.2 -0.118	 0.055 -0.00059 0.055 -0.00091
Multi-peak BGS due to multiple optical modes	Circular core-few mode fiber (FMF) (Li, et al., 2015) LP_{01} LP_{11}	 1.0169 0.99099	 0.05924 0.04872
Multi-peak BGS due to multiple acoustic modes & optical modes	Elliptical core FMF (Fang, et al., 2019) LP_{01}-P_1 LP_{01}-P_2 LP_{11e}-P_1 LP_{11e}-P_2	 1.242 1.278 1.287 1.501	 0.0613 0.0364 0.0658 0.0484
Multiple core/fibers	Different fiber deployment (Bao, et al., 1994)	1.2±0.2	0.054±0.7
	Dual core fiber (Zaghloul, et al., 2018) Core 1 Core 2	 0.971 0.9593	 0.0532 0.0729
	Multicore fiber (MCF) (Mizuno, et al., 2015) Central core Outer core MCF with heterogeneous cores (Zhao, et al., 2017) Central core Outer core	1.08 1.03 1.05±0.095 1.15±0.0343	0.0485 0.0517 0.0485 0.0485
BFS and birefringence	Polarization-maintaining photonic crystal fiber (PM-PCF) (Zhang, et al., 2017) Birefringence	 -40℃ to -15℃: 27.4	 -0.154

	BFS	-15°C to 5°C: 8 5°C to 80°C: 0 1.15	 0.049
BFS and fluorescence	Erbium-doped optical fiber (Ding, et al., 2014) Fluorescence intensity ratio BFS	5.6×10^{-4}/°C 0.87	0 0.0479
Athermal/atensic optical fibers	Highly Ge dope fibers (Deroh, et al., 2019)	0.07	0.0214

The multiple peaks in the BGS observed in specialty fibers exhibit different strain and temperature sensitivities, which enables the construction of the sensor matrix for discriminative sensing. The first measurement of dependence of strain and temperature in PCF was reported in (Zou, et al., 2004). The principles of producing multiple peaks in the BGS are summarized below. Firstly, the multiple peaks of BGS are due to the non-zero overlapping between multiple acoustic modes and the fundamental optical mode, as reported in PCFs with a partially germanium-doped core (Zou, et al., 2003; Zou, et al., 2004), and in large effective-area fiber (LEAF) (Liu & Bao, 2012). Secondly, the interaction between multiple optical modes and the fundamental acoustic modes results in multiple peaks in the BGS as well, as observed in (Li, et al., 2015). Thirdly, choosing proper optical-acoustic mode pairs in an elliptical-core FMF (Fang, et al., 2019) from the interaction between higher order optical modes and higher order acoustic modes can be another alternative approach to optimize the sensing performance of temperature and strain discrimination in BOTDA.

Combination of BFS sensing and other parameter sensing is another effective approach. Polarization-maintaining photonic crystal fiber (PM-PCF) was employed in the sensing system to perform monitoring of BFS and birefringence simultaneously and reported discrimination accuracy of 3 $\mu\varepsilon$ and 0.08 °C (Zou, et al., 2009). Combining BFS and fluorescence measurement was reported in erbium-doped optical fiber-based sensing system to demonstrate strain and temperature discriminative sensing (Ding, et al., 2014). Lastly, temperature-free strain sensing or strain-free temperature sensing could be possible if the sensing fibers are immune to one parameter only. As reported in (Deroh, et al., 2019), highly Ge doped fibers exhibit negligible temperature sensitivity if the fiber coating is removed, presenting a good potential for single parameter sensing. However, the attempts to create athermal or atensic fibers by optimizing the composition of fiber materials encounter a substantial decrease in sensitivity to strain or temperature, as well as in Brillouin gain (Dragic & Ballato, 2018).

Multiplexed distributed fiber sensing system: Firstly, hybrid Brillouin-Rayleigh sensing systems are attracting attention as they are capable of dual parameter measurements for strain and temperature.

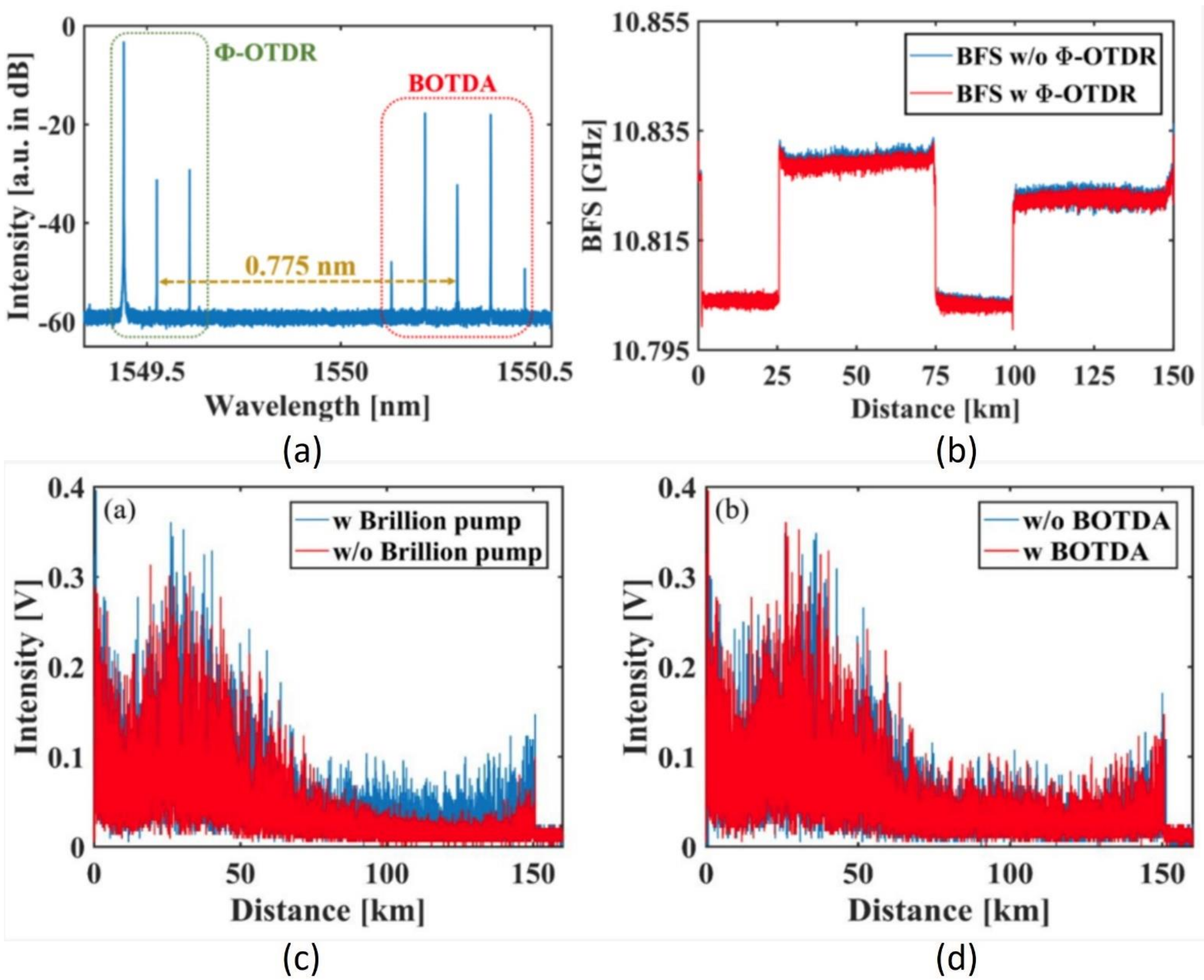

Figure 2: (a) Optical spectrum of the hybrid sensing signals; (b) BFS with/without the Φ-OTDR; (c)Φ-OTDR intensity traces with/without the Brillouin pump; (d) Φ-OTDR intensity traces the operation of BOTDA [Reprinted/Adapted] with permission from *(Fu, et al., 2018).*

In this hybrid system, standard single mode fibers can be used as sensing fiber. Hybrid Brillouin-Rayleigh sensing system was also reported to overcome the challenges of complex interplay among scattering effects inside fiber, the interaction of two sensing signals, and the competition of pump power. Frequency division multiplexing (FDM), wavelength division multiplexing (WDM), and time division multiplexing (TDM) are fused in the system to achieve ultra-long sensing range of 150.62 km, spatial resolution of 9m by BOTDA, and 30m by Φ-OTDR respectively. As depicted in Fig.2, the Φ-OTDR has little impact on the BFS sensing results of BOTDA. Likewise, the Rayleigh scattering signals in the system showed little difference by comparing the intensity trace with and without Brillouin pump, and with/without BOTDA (Fu, et al., 2018). To achieve compact hybrid Brillouin-Rayleigh sensing system, multicore fibers provide spatially separated sensing channels based on the central core and an outer core within the same fiber, for BOTDA and Φ-OTDR, respectively. The hybrid sensing system achieved a good combination of large measurement range of 10 °C by BOTDA, and small resolution of ~0.001 °C by Φ-OTDR (Dang, et al., 2017). This combination represents a promising approach to tackle such trade-off challenges in the sensing system.

Secondly, hybrid Brillouin-Raman sensing systems are developed for distributed sensing of temperature and strain, employing promising techniques based on pulse coding in mitigating the challenges associated with the tradeoff between sensing distance and spatial resolution (Muanenda, et al., 2019).

Selected applications by specialty fiber enabled BOTDA sensing: The BFS difference produced by the central core and outer core presents a desirable opportunity of using multicore fibers for curvature sensing and shape reconstruction (Zhao, et al., 2016). Ring core fibers are another candidate for curvature sensing. Being more bend resistant than SMF, RCF enables distributed curvature sensing with BFS ~ 32.9 MHz for a radius of 0.5 cm, without temperature or axial strain sensitivity by measuring its Brillouin gain variation (Shen, et al., 2020). Optical fibers with double layer polymer coatings are used to enhance the hydrostatic pressure sensitivity and demonstrated for sensitivity-enhanced distributed hydrostatic pressure sensing based on BOTDA. Four kinds of fibers, including single layer coated, double layer coated fiber with outer layer radius of 450, 1000, and 1500 μm were experimentally demonstrated to achieve BFS pressure sensitivity of −0.75 MHz/MPa, −1.65 MHz/MPa, −2.66 MHz/MPa and −3.61 MHz/MPa in the range of 0-30 MPa after temperature compensation, respectively (Dong, et al., 2020). Dynamic pressure measurement based on frequency-agile fast BOTDA and the sensing fiber with double layer coating was demonstrated with promising sensing performance, including static pressure sensitivity of -3.46 MHz/MPa in the range of 0-30 MPa, and large dynamic pressure range with sampling rate of 33.3 KHz, maximum sensing distance of 25 m, and uncertainty of dynamic pressure measurement system is 0.03 MPa (Qiu, et al., 2021). GeO2-doped SMF and pure silica PCF based BOTDA systems for high temperature sensing up to 1100°C and 1200°C are demonstrated, showing measurement accuracy as high as ±2.4°C for the SMF and ±3.6°C for the PCF (Xu, et al., 2016). An annealed single mode gold-coated optical fiber was tested for temperature and strain measurement at high temperatures up to 1000ºC as shown in Fig. 3. The strain coefficient changed from ~0.046 MHz/με at 100 ºC to ~0.022 MHz/με at 1000 °C, mainly due to the increase in Young's modulus of silica with temperature (Xu, et al., 2018). Potential applications of distributed high-temperature strain sensing include asset structural integrity monitoring based on strain monitoring in high temperature environments such as power plants and jet engines.

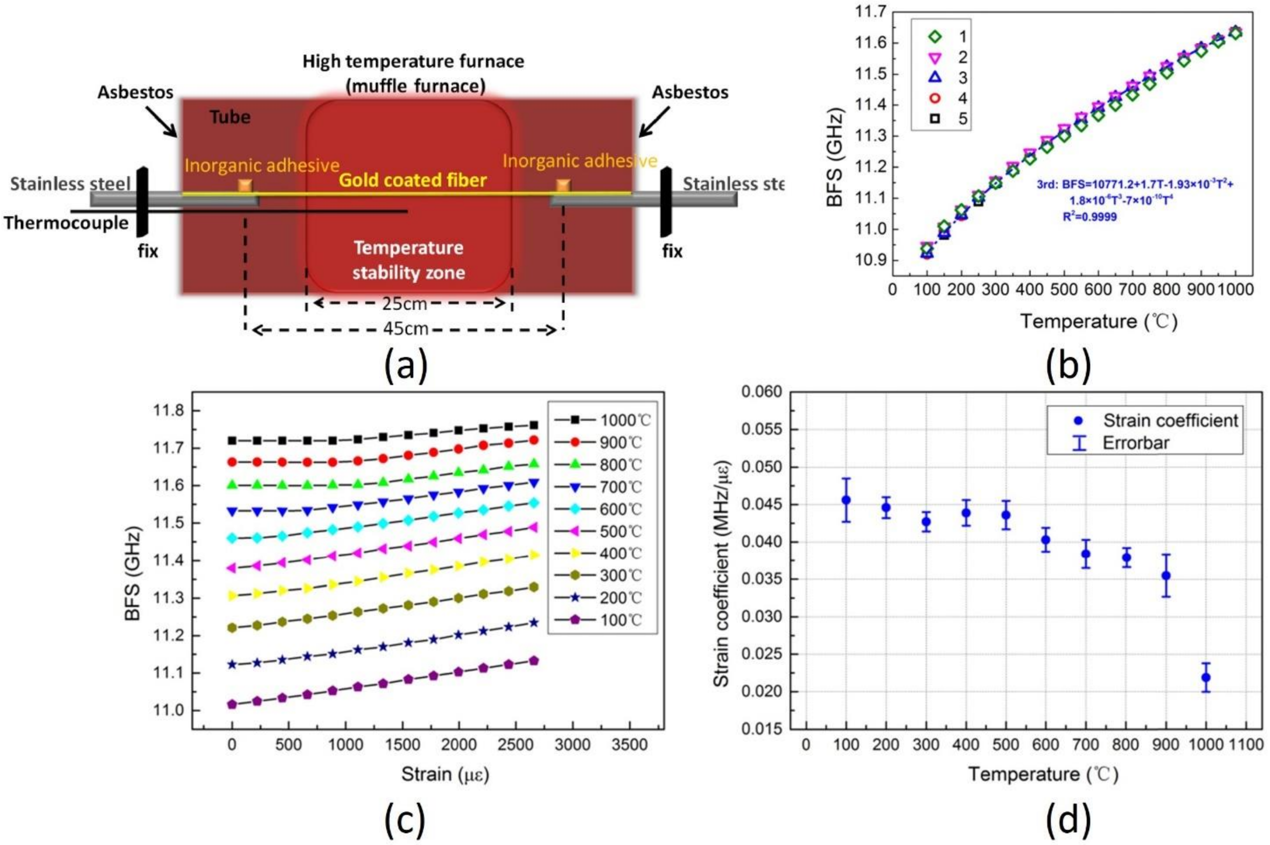

Figure 3: (a) Experimental setup of gold-coated fiber for high-temperature strain measurement with a spatial resolution of 5 cm. (b) 5 measurements of a single sensing point from 100 to 1000 °C with a step of 50 °C, temperature coefficient of gold-coated fiber changes with temperature nonlinearly; High-temperature strain coefficients of annealed gold-coated fiber from 100 to 1000°C. (c) BFS with strain at a position of 3.6 m; (d) strain coefficients for all the data in a span of 25 cm [Reprinted/Adapted] with permission from *(Xu, et al., 2018)* © Optical Society of America.

Outlook and Conclusion

This chapter highlights various achievements utilizing specialty fibers in BOTDA systems, covering key aspects such as the unique properties of large sensitivities, large scale strain introduced by special material into the sensing fiber, sensitivity improvements through specially coated optical fibers, discriminative sensing of temperature and strain, and realization of novel sensing parameters enabled by specialty fibers. It is increasingly recognized that specialty fibers play a crucial role in the design and implementation of BOTDA systems for distributed sensing applications. Additionally, the ongoing development of specialty fibers tailored for sensing applications, achieved through optimization of topology (core shape, number of modes, multi-cores) and the incorporation of material properties (silica/air, gas, highly Ge-doped), such as multi-material fibers, holds the promise of opening new avenues for further enhancing BOTDA system performance.

References

Abedin, K. S., 2005. Observation of strong stimulated Brillouin scattering in single-mode As2Se3 chalcogenide fiber. *Optics Express,* 13(25), pp. 10266-10271.

Bai, Z. et al., 2018. Stimulated Brillouin scattering materials, experimental design and applications: A review. *Optical Materials,* Volume 75, pp. 626-645.

Bao, X. & Chen, L., 2011. Recent Progress in Brillouin Scattering Based Fiber Sensors. *Sensors,* Volume 11, pp. 4252-4287.

Bao, X., Webb, D. J. & Jackson, D. A., 1993. 32-km distributed temperature sensor based on Brillouin loss in an optical fiber. *Optics Letters,* 18(18), pp. 1561-1563.

Bao, X., Webb, D. J. & Jackson, D. A., 1994. Combined distributed temperature and strain sensor based on Brillouin loss in an optical fiber. *Optics Letters,* 19(2), pp. 141-143.

Bastianini, F. et al., 2019. Optical Fiber Sensing Cables for Brillouin-Based Distributed Measurements. *Sensors,* 19(23), p. 5172.

Beugnot, J.-C.et al., 2014. Reduction and control of stimulated Brillouin scattering in polymer-coated chalcogenide optical microwires. *Optics Letters,* 39(3), pp. 482-485.

Beugnot, J.-C.et al., 2007. Complete experimental characterization of stimulated Brillouin scattering in photonic crystal fiber. *Optics Express,* 15(23), pp. 15517-15522.

Brillouin, L., 1922. Diffusion de la lumière et des rayons X par un corps transparent homogène. *Annals of Physics,* 9(17), pp. 88-122.

Cao, D.-F.et al., 2019. Characterization of Soil Moisture Distribution and Movement Under the Influence of Watering-dewatering Using AHFO and BOTDA Technologies. *Environmental & Engineering Geoscience,* 25(3), pp. 189-202.

Chiao, R. Y., Townes, C. H. & Stoicheff, B. P., 1964. Stimulated Brillouin scattering and coherent generation of intense supersonic waves. *Phys. Rev. Lett.,* 12(21), p. 592–595.

Dang, Y. et al., 2017. Towards large dynamic range and ultrahigh measurement resolution in distributed fiber measurement resolution in distributed fiber. *Optics Express,* 25(17), pp. 20183-20193.

Deroh, M. et al., 2020. Comparative analysis of stimulated Brillouin scattering at 2-μm in various infrared glass-based optical fibers. *Journal of the Optical Society of America B,* 37(12), pp. 3792-3800.

Deroh, M. et al., 2019. Towards athermal Brillouin strain sensing based on heavily germania-doped core optical fibers. *APL Photonics,* Volume 4, p. 030801.

Ding, M., Hayashi, N., Mizuno, Y. & Nakamura, K., 2013. Brillouin gain spectrum dependences on temperature and strain in erbium-doped optical fibers with different erbium concentrations. *Applied Physics Letters,* 102(19), p. 191906.

Ding, M., Mizuno, Y. & Nakamura, K., 2014. Discriminative strain and temperature measurement using Brillouin scattering and fluo-rescence in erbium-doped optical fiber. *Optics Express,* 22(20), pp. 24706-24712.

Dong, Y., 2021. High-Performance Distributed Brillouin Optical Fiber Sensing. *Photonics Sensors,* 11(1), p. 69–90.

Dong, Y. et al., 2020. Sensitivity-Enhanced Distributed Hydrostatic Pressure Sensor Based on BOTDA in Single-Mode Fiber With Double-Layer Polymer Coatings. *Journal of Lightwave Technology,* 38(8), pp. 2564-2571.

Dong, Y. et al., 2014. Characterization of evolution of mode coupling in a graded-index polymer optical fiber by using Brillouin optical time-domain analysis. *Optics Express,* 22(22), pp. 26510-26516.

Dragic, P. & Ballato, J., 2018. A Brief Review of Specialty Optical Fibers for Brillouin-Scattering-Based Distributed Sensors. *Applied Sciences,* 8(10), p. 1996.

E. P. Ippen, R. H. S., 1972. Stimulated Brillouin scattering in optical fibers. *Applied Physics Letters,* Volume 21, p. 539.

Fang, J. et al., 2019. Multi-parameter distributed fiber sensing with higher-order optical and acoustic modes. *Optics Letters,* 44(5), pp. 1096-1099.

Feng, C., Kadum, J. E. & Schneider, T., 2019. The State-of-the-Art of Brillouin Distributed Fiber Sensing. In: *Fiber Optic Sensing - Principle, Measurement and Applications.* s.l.:intechopen, p. 84684.

Florea, C. et al., 2006. Stimulated Brillouin scattering in single-mode As2S3 and As2Se3 chalcogenide fibers. *Optics Express,* 14(25), pp. 12063-12070.

Fortier, C. et al., 2008. Experimental investigation of Brillouin and Raman scattering in a 2SG sulfide glass microstructured chalcogenide fiber. *Optics Express,* 16(13), pp. 9398-9404.

Fu, Y. et al., 2018. Ultra-Long-Distance Hybrid BOTDA/Φ-OTDR. *Sensors,* Volume 18, p. 976.

Galindez, C., Madruga, F. J. & Lopez-Higuera, J. M., 2008. Influence of Humidity on the Measurement of Brillouin Frequency Shift. *IEEE Photonics Technology Letters,* 20(23), pp. 1959 - 1961.

Gao, S. et al., 2022. Monitoring local temperature and longitudinal strain along a nonuniform As2Se3-PMMA tapered fiber by Brillouin gain-profile tracing. *Optics Express,* 30(16), pp. 29655-29664.

Gu, H. et al., 2013. Effects of Polymer Coatings on Temperature Sensitivity of Brillouin Frequency Shift Within Double-Coated Fibers. *IEEE Sensors Journal,* 13(2), pp. 864-869.

Guo, T. et al., 2009. Experimental study on strain and deformation monitoring of reinforced concrete structures using PPP-BOTDA. *Science in China Series E: Technological Sciences,* Volume 59, pp. 2859-2868.

Hayashi, N., Minakawa, K., Mizuno, Y. & Nakamura, K., 2014. Brillouin frequency shift hopping in polymer optical fiber. *Applied Physics Letters,* 105(9), p. 091113.

Hayashi, N., Mizuno, Y. & Nakamura, K., 2012. Brillouin gain spectrum dependence on large strain in perfluorinated graded-index polymer optical fiber. *Optics Express,* 20(19), pp. 21101-21106.

Horiguchi, T., Kurashima, T. & Tateda, M., 1989. Tensile strain dependence of Brillouin frequency shift in silica optical fibers. *IEEE Photonics Technology Letters,* 1(5), pp. 107-108.

Hu, D. J. J. et al., 2021. Review of specialty fiber based Brillouin optical time domain analysis technology. *Photonics,* 8(10), p. 421.

Iten, M., Hauswirth, D. & Puzrin, A., 2011. *Distributed fiber optic sensor development, testing, and evaluation for geotechnical monitoring applications.* San Diego, California, United States, s.n.

Kobyakov, A., Sauer, M. & Chowdhury, D., 2010. Stimulated Brillouin scattering in optical fibers. *Advances in Optics and Photonics,* 2(1), pp. 1-59.

Kurashima, T., Horiguchi, T. & Tateda, M., 1990. Thermal effects of Brillouin gain spectra in single-mode fibers. *IEEE Photonics Technology Letters,* 2(10), pp. 718-720.

Kwon, I.-B.et al., 2009. *Feasibility study for monitoring of offshore pipelines using BOTDA system.* Orlando, Florida, United States, s.n.

Lee, J. H. et al., 2005. Experimental comparison of a Kerr nonlinearity figure of merit including the stimulated Brillouin scattering threshold for state-of-the-art nonlinear optical fibers. *Optics Letters,* 30(13), pp. 1698-1700.

Li, A. et al., 2015. Few-mode fiber multi-parameter sensor with distributed temperature and strain discrimination. *Optics Letters,* 40(7), pp. 1488-1491.

Liu, H. et al., 2023. Specialty optical fibers for advanced sensing applications. *Opto-Electronic Science,* Volume 2, p. 220025.

Liu, X. & Bao, X., 2012. Brillouin spectrum in leaf and simultaneous temperature and strain measurement. *Journal of Lightwave Technology,* 30(8), pp. 1053 - 1059.

Liu, Y. et al., 2021. Damage detection of tunnel based on the high-density cross-sectional curvature obtained using strain data from BOTDA sensors. *Mechanical Systems and Signal Processing,* Volume 158, p. 107728.

Lu, X., Soto, M. A. & Thévenaz, L., 2017. Impact of the Fiber Coating on the Temperature Response of Distributed Optical Fiber Sensors at Cryogenic Ranges. *Journal of Lightwave Technology,* 36(4), pp. 961-967.

Minakawa, K. et al., 2016. Dependence of Brillouin frequency shift on water absorption ratio in polymer optical fibers. *Journal of Applied Physics,* 119(22), p. 223102.

Minakawa, K., Mizuno, Y. & Nakamura, K., 2017. Cross Effect of Strain and Temperature on Brillouin Frequency Shift in Polymer Optical Fibers. *Journal of Lightwave Technology,* 35(12), pp. 2481 - 2486.

Mizuno, Y. et al., 2015. Brillouin scattering in multi-core optical fibers for sensing applications. *Scientific Reports,* Volume 5, p. 11388.

Mizuno, Y., He, Z. & Hotate, K., 2009. Dependence of the Brillouin frequency shift on temperature in a tellurite glass fiber and a bismuth-oxide highly-nonlinear fiber. *Applied Physics Express,* 2(11), p. 112402.

Mizuno, Y., He, Z. & Hotate, K., 2010. Distributed strain measurement using a tellurite glass fiber with Brillouin optical correlation-domain reflectometry. *Optics Communications,* 283(11), pp. 2438-2441.

Mizuno, Y., Lee, H., Hayashi, N. & Nakamura, K., 2018. Hydrostatic pressure dependence of Brillouin frequency shift in polymer optical fibers. *Applied Physics Express,* 11(1), p. 012502.

Mizuno, Y. et al., 2018. Brillouin characterization of slimmed polymer optical fibers for strain sensing with extremely wide dynamic range. *Optics Express,* 26(21), pp. 28030-28037.

Mizuno, Y. & Nakamura, K., 2010. Experimental study of Brillouin scattering in perfluorinated polymer optical fiber at telecommunication wavelength. *Applied Physics Letters,* 97(2), p. 021103.

Mizuno, Y. & Nakamura, K., 2010. Potential of Brillouin scattering in polymer optical fiber for strain-insensitive high-accuracy temperature sensing. *Optics Letters,* 35(23), pp. 3982-3987.

Mizuno, Y. et al., 2021. Distributed polymer optical fiber sensors: a review and outlook. *Photonics Research,* 9(9), pp. 1719-1733.

Motil, A., Bergman, A. & Tur, M., 2016. State of the art of Brillouin fiber-optic distributed sensing. *Optics & Laser Technology,* Volume 78, pp. 81-103.

Muanenda, Y., Oton, C. J. & Pasquale, F. D., 2019. Application of Raman and Brillouin Scattering Phenomena in Distributed Optical Fiber Sensing. *Frontiers in Physics,* Volume 7, p. 155.

Niklès, M., Thévenaz, L. & Robert, P. A., 1996. Simple distributed fiber sensor based on Brillouin gain spectrum analysis. *Optics Letters,* 21(10), pp. 758-760.

Qiu, L. et al., 2021. Dynamic Distributed Pressure Measurement Using Frequency-Agile Fast BOTDA. *IEEE Sensors Journal,* 21(22), pp. 25743 - 25748.

Saxena, B., Baker, C., Bao, X. & Chen, L., 2019. High birefringent Brillouin frequency shifts in a single-mode As2Se3-PMMA microtaper induced by a transverse load. *Optics Letters,* 44(19), pp. 4789-4792.

Saxena, B., Baker, C., Bao, X. & Chen, L., 2019. Simultaneous generation of guided-acoustic-wave Brillouin scattering and stimulated-Brillouin-scattering in hybrid As2Se3-PMMA microtapers. *Optics Express,* 27(10), pp. 13734-13743.

Schreier, A., Liehr, S., Wosniok, A. & Krebber, K., 2018. Investigation on the Influence of Humidity on Stimulated Brillouin Backscattering in Perfluorinated Polymer Optical Fibers. *Sensors,* 18(11), p. 3952.

Schreier, A., Wosniok, A., Liehr, S. & Krebber, K., 2018. Humidity-induced Brillouin frequency shift in perfluorinated polymer optical fibers. *Optics Express,* 26(17), pp. 22307-22314.

Shen, L. et al., 2020. Distributed curvature sensing based on a bending loss-resistant ring-core fiber. *Photonics Research,* 8(2), pp. 165-174.

Song, K. Y. et al., 2006. Highly efficient Brillouin slow and fast light using As2Se3 chalcogenide fiber. *Optics Express,* 14(13), p. 5860–5865.

T.Horiguchi, T.Kurashima & M.Tateda, 1990. A technique to measure distributed strain in optical fibers. *IEEE Photonics Technology Letters,* 2(5), pp. 352-354.

Wang, H., Baker, C., Chen, L. & Bao, X., 2021. Stimulated Brillouin scattering in high-birefringence elliptical-core As2Se3-PMMA microfibers. *Optics Letters,* 46(5), pp. 945-948.

Wang, H. et al., 2020. Stimulated Brillouin scattering in a tapered dual-core As2Se3-PMMA fiber for simultaneous temperature and strain sensing. *Optics Letters,* 45(12), pp. 3301-3304.

Wang, H. et al., 2020. Wide-range strain sensor based on Brillouin frequency and linewidth in an As2Se3-PMMA hybrid microfiber. *Optics Express,* 28(15), pp. 22933-22945.

Xu, P. et al., 2018. Distributed Brillouin optical fiber temperature and strain sensing at a high temperature up to 1000 °C by using an annealed gold-coated fiber. *Optics Express,* 26(23), pp. 29724-29734.

Xu, P. et al., 2016. 1200°C high-temperature distributed optical fiber sensing using Brillouin optical time domain analysis. *Applied Optics,* 55(21), pp. 5471-5478.

Yang, F., Gyger, F. & Thévenaz, L., 2020. Giant Brillouin Amplification in Gases. *Optics and Photonics News,* 31(12), pp. 33-33.

Yang, F., Gyger, F. & Thévenaz, L., 2020. Intense Brillouin amplification in gas using hollow-core waveguides. *Nature Photonics,* Volume 14, pp. 700-708.

Zaghloul, M. A. et al., 2018. Discrimination of Temperature and Strain in Brillouin Optical Time Domain Analysis Using a Multicore Optical Fiber. *Sensors,* 18(4), p. 1176.

Zhang, D. et al., 2020. Structural Crack Detection Using DPP-BOTDA and Crack-Induced Features of the Brillouin Gain Spectrum. *Sensors,* 20(23), p. 6947.

Zhang, H. et al., 2017. Simultaneous measurement of strain and temperature using a polarization-maintaining photonic crystal fiber with stimulated Brillouin scattering. *Applied Physics Express,* Volume 10, p. 012501.

Zhang, S., Liu, B. & He, J., 2019. Pipeline deformation monitoring using distributed fiber optical sensor. *Measurement,* Volume 133, pp. 208-213.

Zhao, Z. et al., 2017. Spatial-division multiplexed Brillouin distributed sensing based on a heterogeneous multicore fiber. *Optics Letters,* 42(1), pp. 171-174.

Zhao, Z., Soto, M. A., Tang, M. & Thévenaz, L., 2016. Distributed shape sensing using Brillouin scattering in multi-core fibers. *Optics Express,* 24(22), pp. 25211-25223.

Zou, L., Bao, X. & Chen, L., 2003. Brillouin scattering spectrum in photonic crystal fiber with a partially germanium-doped core. *Optics Letters,* 28(21), pp. 2022-2024.

Zou, L., Bao, X., V., S. A. & Chen, L., 2004. Dependence of the brillouin frequency shift on strain and temperature in a photonic crystal fiber. *Optics Letters,* 29(13), pp. 1485-1487.

Zou, L., Bao, X., V, S. A. & Chen, L., 2004. Dependence of the Brillouin frequency shift on strain and temperature in a photonic crystal fiber. *Optics Letters,* 29(13), pp. 1485-1487.

Zou, W., He, Z. & Hotate, K., 2009. Complete discrimination of strain and temperature using Brillouin frequency shift and birefringence in a polarization-maintaining fiber. *Optics Express,* 17(3), pp. 1248-1255.

Index terms

Brillouin optical time domain analysis (BOTDA)

Specialty fibers

Template

Photonic crystal fibers (PCFs)

Brillouin frequency shift (BFS)

Brillouin gain spectrum (BGS)

Polymer fibers

Tellurite fibers

Bismuth-oxide fibers

Erbium-doped fibers

As2Se3-PMMA fibers

Few mode fibers (FMFs)

Multicore fibers